Current Biology, Volume *23*

A Matrix Protein Silences Transposons and Repeats through Interaction with Retinoblastoma-Associated Proteins

Yifeng Xu, Yizhong Wang, Hume Stroud, Xiaofeng Gu, Bo Sun, Eng-Seng Gan, Kian-Hong Ng, Steve. E. Jacobsen, Yuehui He, and Toshiro Ito

Supplemental Inventory

Figure S1. (Related to Figure 1).

Expression levels of *TEK* homologs in various Arabidopsis tissues.

Figure S2. (Related to Figure 1).

Reduction in *TEK* mRNA levels in *35S::amiTEKa* and *35S::amiTEKb* are correlated with late-flowering phenotypes.

Figure S3. (Related to Figure 2).

TEK binds to the *FLC* locus and mediates histone modification.

Figure S4. (Related to Figure 3).

TEK affects DNA methylation and histone modification at *AtMu1* and *FWA*.

Table S1.

Microarray screening data of upregulated and downregulated genes in *amiTEK* seedling at day 5 after germination compared to the ones in the wild-type L*er* background ($p<0.05$ cutoff).

Table S2.

RNA-sequencing data of transposons upregulated over 4 fold in the inflorescences of introgressed *tek-1* compared to the ones in the wild-type L*er* ($p<0.05$ cutoff).

Table S3.

RNA-sequencing data of protein-coding genes upregulated over 4 fold in the inflorescences of introgressed *tek-1* compared to the wild-type L*er* ($p<0.05$ cutoff). Upregulated genes overlapping with the ones in *amiTEK* are shown in red.

Table S4.

Oligonucleotide sequences used in this study.

Figure S1

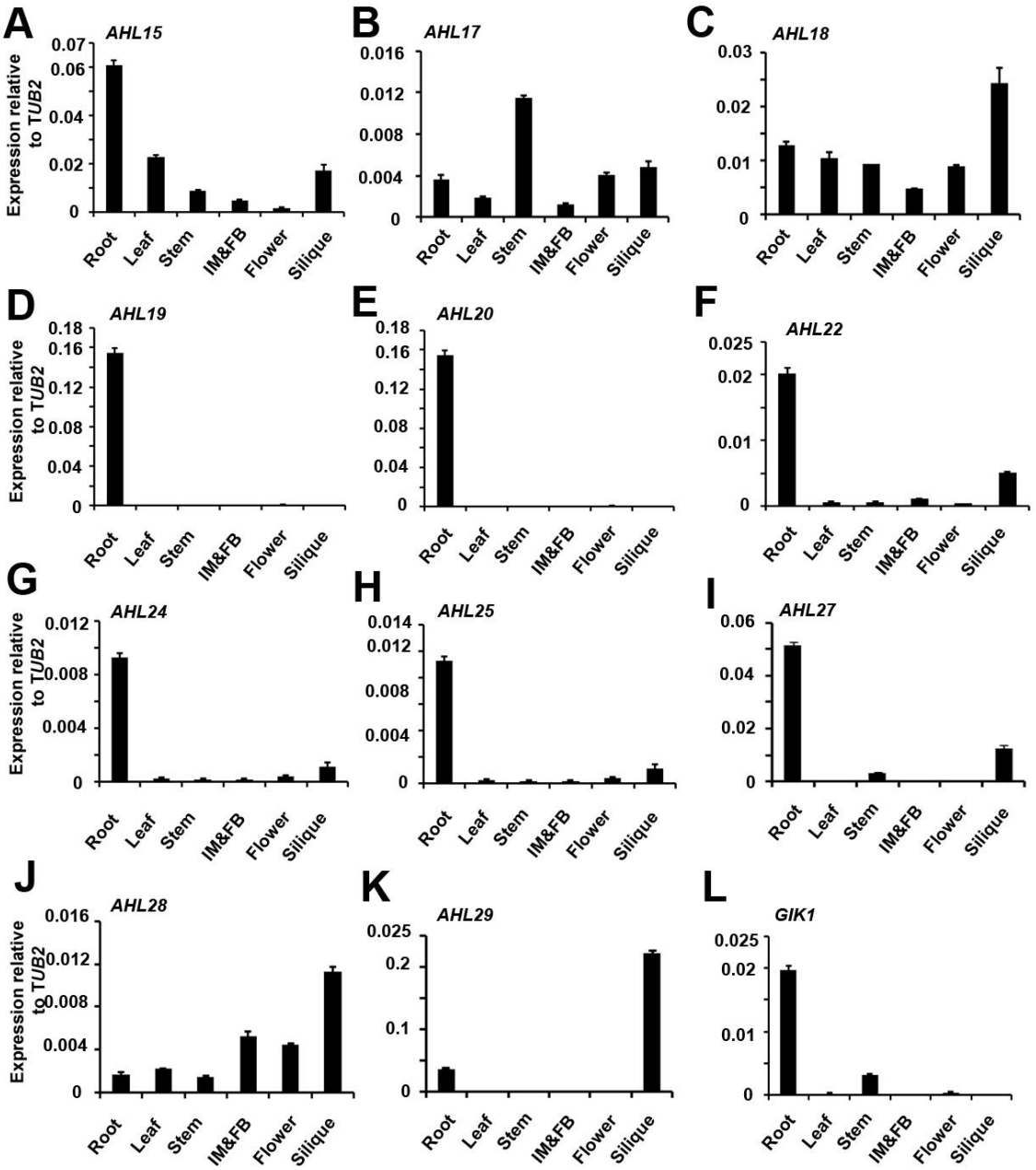
A
AHL15
B
AHL17
C
AHL18
D
AHL19
E
AHL20
F
AHL22
G
AHL24
H
AHL25
I
AHL27
J
AHL28
K
AHL29
L
GIK1
Expression relative to TUB2
Root
Leaf
Stem
IM&FB
Flower
Silique

Figure S1. (Related to Figure 1). Expression levels of *TEK* homologs in various Arabidopsis tissues.

(A-L) The expression levels of *TEK* homologs relative to expression level of *TUBULIN2* (*TUB2*) are shown. The tissues tested include root, leaf (as shown in figure), stem, inflorescence meristem and young floral bud (IM&FB), flower and silique. All the error bars show the standard deviation based on three biological replicates

Figure S2

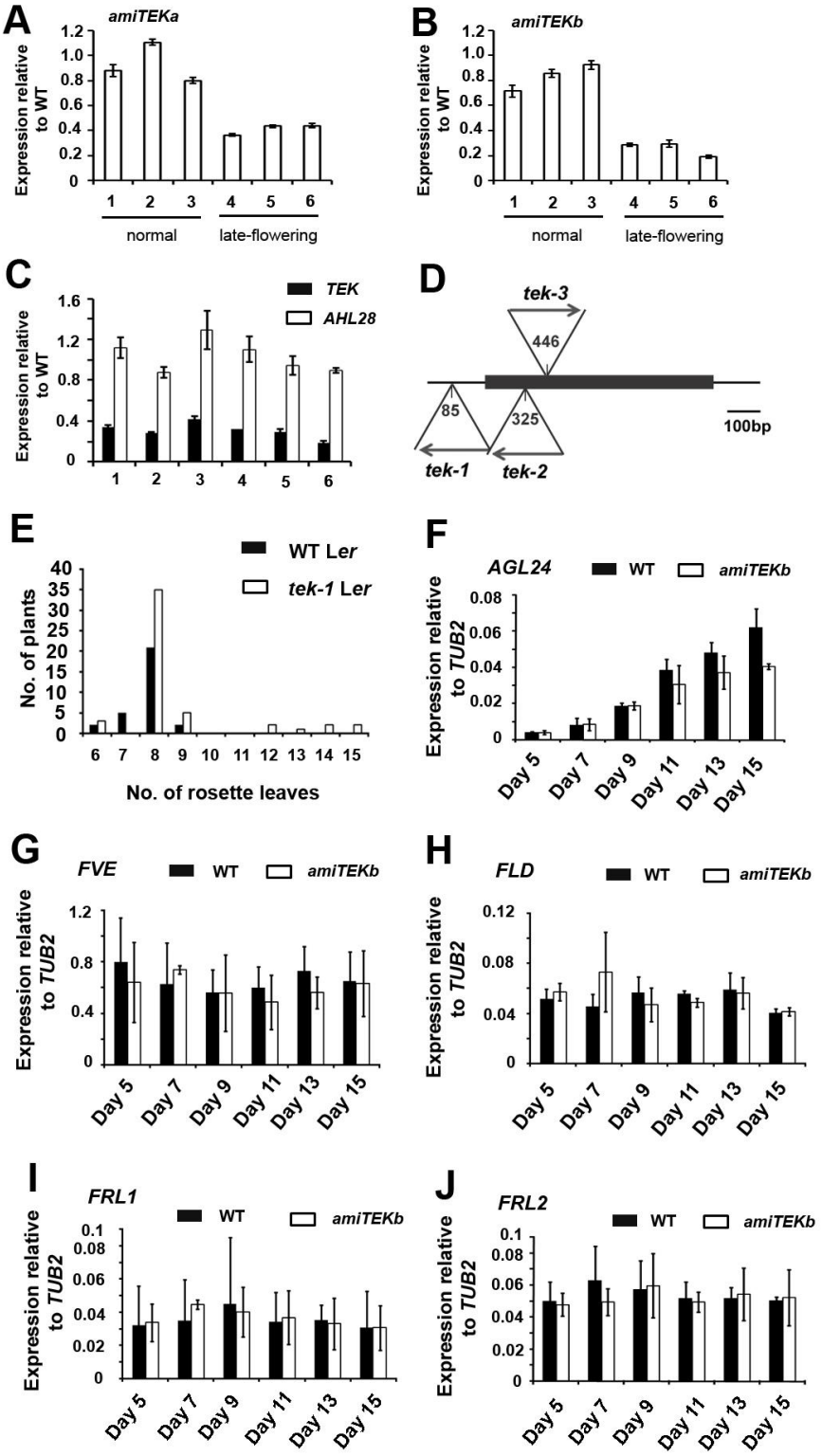
A
amiTEKa
Expression relative to WT
normal
late-flowering
B
amiTEKb
C
TEK
AHL28
D
tek-3
446
85
325
100bp
tek-1
tek-2
E
WT Ler
tek-1 Ler
No. of plants
No. of rosette leaves
F
AGL24
WT
amiTEKb
Expression relative to TUB2
G
FVE
H
FLD
I
FRL1
J
FRL2
Day 5
Day 7
Day 9
Day 11
Day 13
Day 15

Figure S2. (Related to Figure 1). Reduction in *TEK* mRNA levels in *35S::amiTEKa* and *35S::amiTEKb* are correlated with late-flowering phenotypes.

(A-B) *35S::amiTEKa* (A) and *35S::amiTEKb* (B) specifically knocked down *TEK* at different levels. The inflorescences of the wild type-like plants (1-3) and the late-flowering plants (4-6) were chosen from independent T1 plants for RNA extraction, cDNA synthesis and real-time PCR assay with primers RT-TEK-F: GCTCGAAATCACTCTTCTAAAGTAGGC and RT-TEK-R: CATCAATCGAAGGAGAG-ATGGCTAAGA. The relative fold changes of *TEK* expression in *35S::amiTEKa* and *35S::amiTEKb* to wild-type plants are shown. In correlation with the delayed flowering phenotypes, the *TEK* mRNA levels were reduced to around 30-45% in *35S::amiTEKa* and around 15-35% in *35S::amiTEKb* plants.

(C) In selected 6 *35S::amiTEKb* plants with the late-flowering phenotypes, while *TEK* was decreased, expression of its homolog *AHL28* was not changed as compared to WT plants.

(D-E) T-DNA insertion lines of *TEK* and segregation of late-flowering phenotypes after crossing with the L*er* wild-type. (D) T-DNA insertions in the *tek-1* allele in the Col background and, *tek-2 and tek-3* alleles in the WS background. The numbering begins from the transcriptional start site. The dark box represents the exon. (E) After four rounds of backcrossing with WT L*er* plants, in the F2 population, around 10% of *tek-1* plants showed late flowering phenotypes, while no plants from WT or the original *tek-1* showed late flowering phenotypes.

(F-J) Relative expression levels of flowering-time genes. (F) The relative expression level of *AGL24* to *TUB2* in flowering. (G-J) The relative expression levels of the putative *FLC* regulators to *TUB2* in flowering. The expression levels of *FVE* (G), *FLD* (H), *FRI-like1/FRL1* (I) and *FRI-like2/FRL2* (J) were not changed significantly in the *amiTEK* plants.

All the error bars show the standard deviation based on three biological replicates

Figure S3

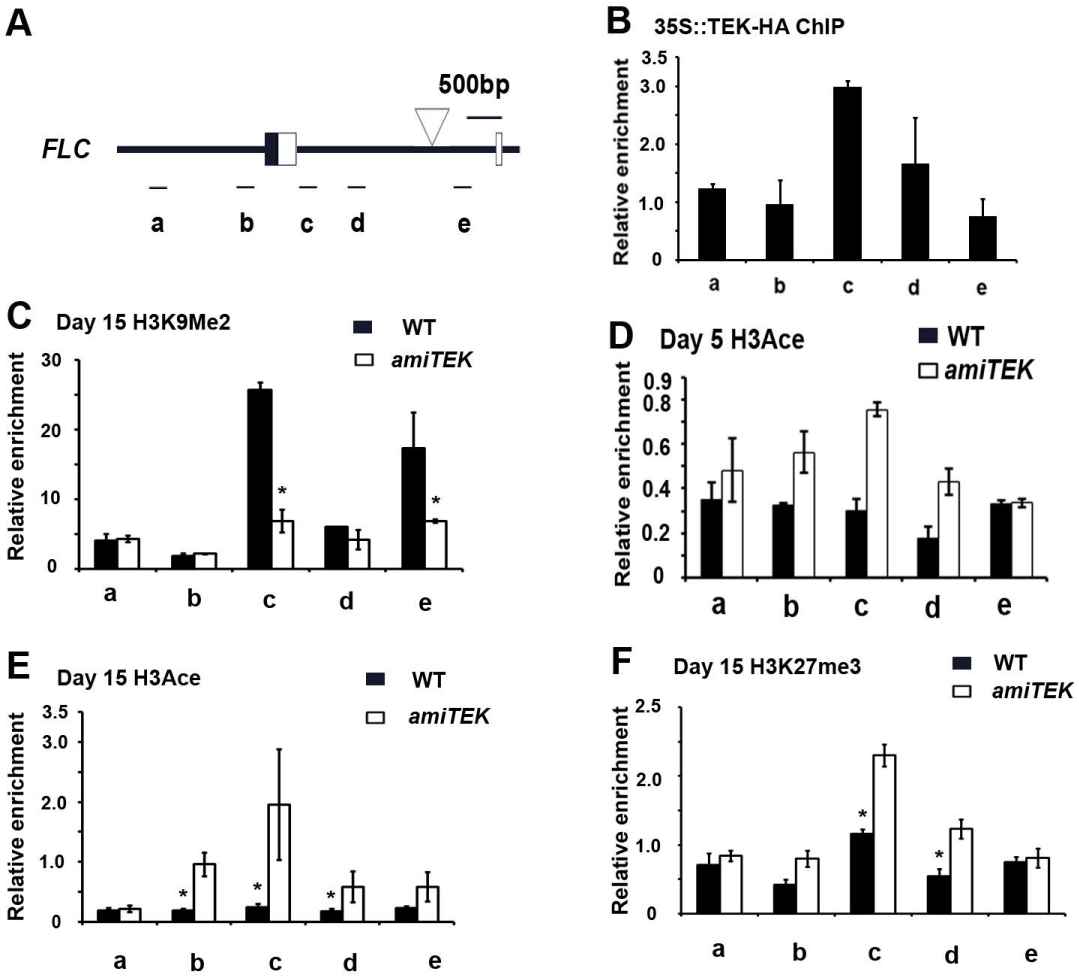
A
500bp
FLC
a
b
c
d
e
B
35S::TEK-HA ChIP
Relative enrichment
C
Day 15 H3K9Me2
WT
amiTEK
Relative enrichment
D
Day 5 H3Ace
WT
amiTEK
Relative enrichment
E
Day 15 H3Ace
WT
amiTEK
Relative enrichment
F
Day 15 H3K27me3
WT
amiTEK
Relative enrichment

Figure S3. (Related to Figure 2). TEK binds to the *FLC* locus and mediates histone modification.

(A) Schematic structure of the *FLC* locus showing the 5' untranslated region (black box) and the first two exons (white boxes). Letters a to e (in panels A-F) represent the amplicons examined by real-time PCR. The location of the 1.2-kb TE insertion in L*er* is shown as a white triangle.

(B) Binding of TEK to the *FLC* locus examined by ChIP assay with the overexpression line *35S::TEK-HA*. The leaves of *35S::TEK-HA* plants in L*er* were used for ChIP with anti-HA antibody. Relative enrichment was standardized to the sample pulled down with the unrelated anti-c-Myc antibody.

(C-F) Relative fold enrichments of epigenetic marks at the *FLC* locus, H3K9 dimethylation (C), H3 acetylation (D, E) and H3K27 trimethylation (F) using the aerial parts of DAG 5 plants (D) and DAG 15 (C, E. F). H3K9 dimethylation levels were much higher at the regions c and e in the WT plants than in *amiTEK* (C) even at DAG 15. In contrast, H3 acetylation levels were much higher in *amiTEK* plants at the wider regions b-e (D, E). H3K27me3 was higher at DAG 15 due to the floral induction in wild-type plants, while it was maintained at a lower level in *amiTEK* plants; the decrease in H3K27me3 is most likely associated with the elevated expression of *FLC* in these plants (F).

All the error bars in (B), (C), (E) and (F) show the standard deviation based on three biological replicates. Figures S3D is a biological replicate of Figures 2E with the standard deviation based on technical replicates and showed the similar trend. Asterisks indicate statistically significant difference (paired Student's *t*-test, $p<0.05$) between samples.

Figure S4

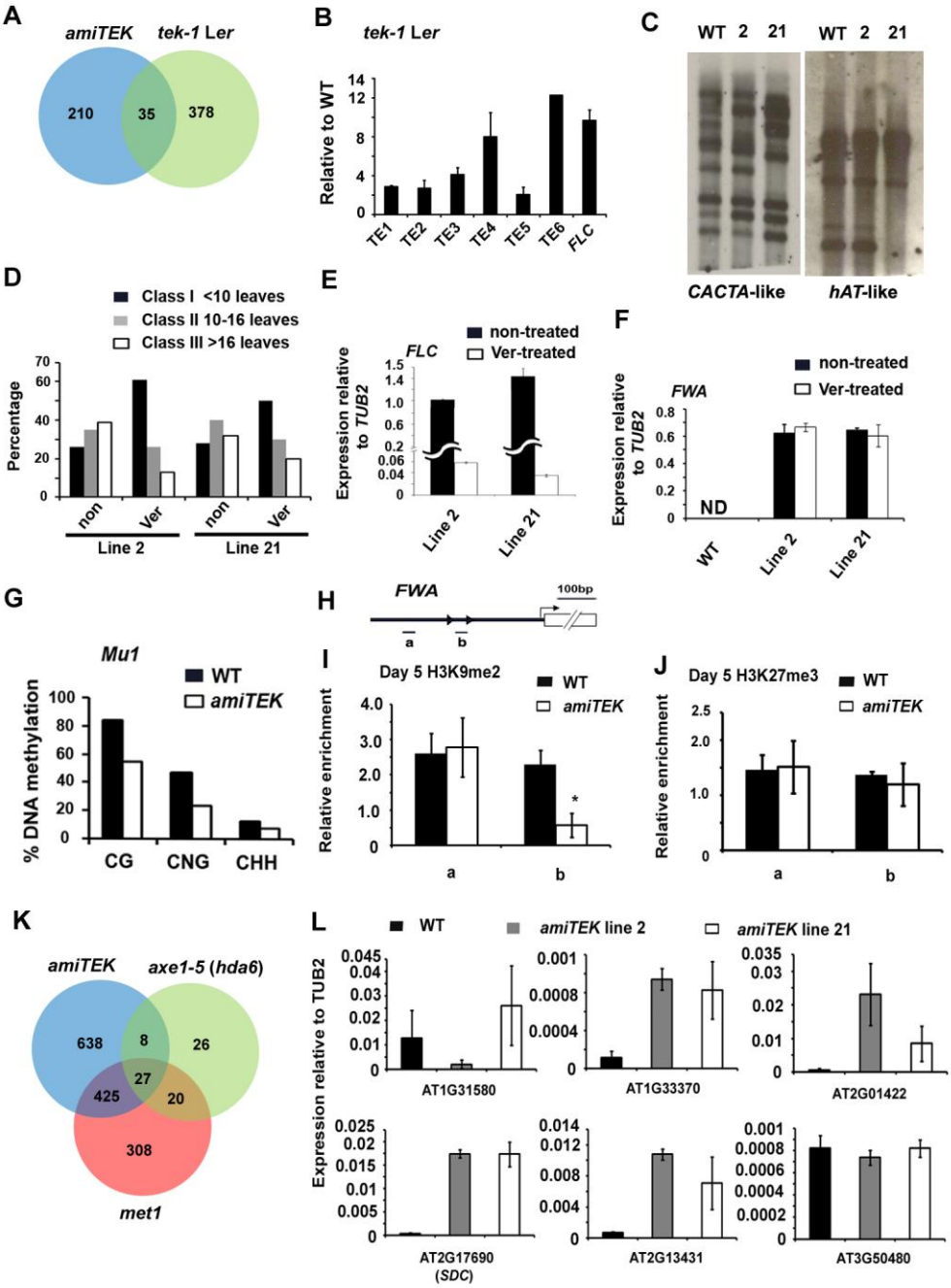
A
amiTEK
tek-1 Ler
210
35
378
B
tek-1 Ler
Relative to WT
TE1
TE2
TE3
TE4
TE5
TE6
FLC
C
WT 2 21
WT 2 21
CACTA-like
hAT-like
D
Class I <10 leaves
Class II 10-16 leaves
Class III >16 leaves
Percentage
non
Ver
non
Ver
Line 2
Line 21
E
FLC
non-treated
Ver-treated
Expression relative to TUB2
Line 2
Line 21
F
FWA
non-treated
Ver-treated
Expression relative to TUB2
ND
WT
Line 2
Line 21
G
Mu1
WT
amiTEK
% DNA methylation
CG
CNG
CHH
H
FWA
100bp
a
b
I
Day 5 H3K9me2
WT
amiTEK
Relative enrichment
a
b
J
Day 5 H3K27me3
WT
amiTEK
Relative enrichment
a
b
K
amiTEK
axe1-5 (hda6)
638
8
26
27
425
20
308
met1
L
WT
amiTEK line 2
amiTEK line 21
Expression relative to TUB2
AT1G31580
AT1G33370
AT2G01422
AT2G17690
(SDC)
AT2G13431
AT3G50480

Figure S4. (Related to Figure 3). *TEK* affects DNA methylation and histone modification at *AtMu1* and *FWA*.

(A) A Venn diagram showing the overlap between the AGI genes upregulated in *amiTEK* seedlings and in *tek-1 (*L*er*) inflorescence. The AGI genes that were transcriptionally upregulated (>4 fold, p-initial<0.05) compared with wild-type plants were used for comparison.

(B) Validation of TE genes upregulated in *tek-1 seedlings* by RT-PCR. Thirteen TE loci that were upregulated in *tek-1* inflorescence identified by RNA-sequencing analysis were selected and the upregulation in six of the TE loci and *FLC* was confirmed by RT-PCR. *TE1* (AT3TE04155), *TE2* (AT1TE56445), *TE3* (AT1TE56445), *TE4* (AT5TE49350), *TE5* (AT3TE41285) and *TE6* (AT4TE21200).

(C) Transposition of *CACTA*-like and *hAT*-like transposons in two independent *amiTEK* lines.

A genomic southern blot showing that the *CACTA*-like *and hAT*-like TEs moved independently in the *amiTEK* lines 2 and 21. The same pair of primers for real-time PCR was used to amplify ~150-bp probes for the hybridization.

(D-F) Two independent *amiTEK* lines (2 and 21) were subjected to a 6-week vernalization treatment. The treatment accelerated flowering but was unable to fully rescue the late-flowering phenotypes of the *amiTEK* plants (D). *FLC* expression was greatly decreased (E). In contrast, *FWA*, which was not expressed in vegetative tissues of the wild-type plants (F, ND, non-detectable), was ectopically expressed in the vegetative tissues of the *amiTEK* plants (F, black bars), but the vernalization treatment did not affect *FWA* (F, white bars).

(G) DNA methylation state of *AtMu1* upon *TEK* knockdown. 19 and 22 plasmids were sequenced for L*er* and *amiTEK*, respectively.

(H-J) ChIP assay for H3K9me2 and H3K27me3 marks at the *FWA* locus at DAG5. Schematic structure of genomic *FWA* (H). In *amiTEK*, the H3K9me2 level was reduced at the SINE-like region of the *FWA* locus (I), but the H3K27me3 level was not changed (J).

(K) A Venn diagram showing the significant overlap between the AGI genes upregulated in *amiTEK*, *axe1-5 (hda6)* and in *met1-3*. The published AGI genes that were transcriptionally upregulated in *axe1-5* [1] and in *met1-3* [2, 3] compared with wild-type plants (>3 fold, p-initial<10^{-6}, FDR α=0.05) were used to compare with the AGI genes upregulated in *amiTEK* (>3 fold, p-initial<10^{-6}*).*

(L) The expression level of reported RdDM targets relative to *TUB2* in Day 5 seedlings of wild-type, lines 2 and 21 *of amiTEK* was shown. Among six texted genes, except AT3G50480, other five genes are obviously increased in at least one *amiTEK* lines, including *SUPPRESSOR OF drm1 drm2 cmt3* (*SDC*, AT2G17690), indicating the cross-talk between TEK function and RdDM pathway.

All the error bars show the standard deviation based on three biological replicates.

Table S1 (Related to Figure 3A). List of Upregulated and Downregulated Genes in *amiTEK*

(See accompanying Excel sheet.)

Excel sheet of microarray screening data of upregulated and downregulated genes in *amiTEK* seedling at day 5 after germination compared to the ones in the wild-type L*er* background ($p<0.05$ cutoff)

Table S2. List of Upregulated Transposons in the Introgressed *tek-1*

(See accompanying Excel sheet.)

Excel sheet of RNA-sequencing data of transposons upregulated over 4 fold in the inflorescences of introgressed *tek-1* compared to the ones in the wild-type L*er* ($p<0.05$ cutoff)

Table S3. List of Upregulated Protein-Coding Genes in the Introgressed *tek-1*

(See accompanying Excel sheet.)

Excel sheet of RNA-sequencing data of protein-coding genes upregulated over 4 fold in the inflorescences of introgressed *tek-1* compared to the wild-type L*er* ($p<0.05$ cutoff). Upregulated genes overlapping with the ones in *amiTEK* are shown in red.

Table S4

Primer Name	Primer Sequence
RT-TUB2-F	ATCCGTGAAGAGTACCCAGAT
RT-TUB2-R	AAGAACCATGCACTCATCAGC
RT-TEK-F	CATCAATCGAAGGAGAGATGGCTAAGA
RT-TEK-R	CTCTGAGGGAATTTGGACTGTCGTGAGT
RT-FLC-F	GATAGCAAGCTTGTGGGATCAAATGTCAAA
RT-FLC-R	CTCAACAAGCTTCAACATGAGTTCGGTC
RT-FWA-F	AGGCAATACTGGTGGAGGATGTCTACTG
RT-FWA-R	GACAATAGTATGAGCCATGAGTGTCTCGAC
RT-FT-F	CCTCAGGAACTTCTATACTTTGGTTATGG
RT-FT-R	CTGTTTGCCTGCCAAGCTGTC
RT-SOC1-F	AGCTGCAGAAAACGAGAAGCTCTCTG
RT-SOC1-R	GGCTACTCTCTTCATCACCTCTTCC
RT-At5G45082-F	ACACTCCACCAATCAACCACAGCGTGTA
RT-At5G45082-R	TCTTGGAAGTTGTTGCCTTGAGACGAG
RT-At5G32306-F	CTGGAGTACGACATGGTTGGCGATTTC
RT-At5G32306-R	CTGAAGTATGGTTGTGGCCTCGATGCAG
RT-At5G43800-F	GGGGAGATTATGGGTTGGTTTCGTCTT
RT-At5G43800-R	CATCAACTGGCGGTACATAGTCGTCATC
RT-At5G33050-F	CTCGACCACACCTTACAAGGACCGAATG
RT-At5G33050-R	CCAGCACCGCTCTGATGATATTCGAC
RT-At2G05700-F	TGCAATGCAAGTGTCATCGGTTGACTCT
RT-At2G05700-R	CTCCGTGCACAACAACACTTCAACCAT
RT-At5G55896-F	TCGCGCAGCTCGTGGTGTACAACCTGT
RT-At5G55896-R	TCGCGATCAACTAAACGAAAGACCACCG
RT-At1G33460-F	CCCAACAGTTTGCACACCTTCGAGGCTAT
RT-At1G33460-R	CCGGTTGAAGACATCATTCTCGTTTGCATC
Probe-FLC-TE-F	CTTCGTTCTTTTTCTCTCCTTC
Probe-FLC-TE-R	CGCTTCTAGATCTAAGAATGATC
GT-FLC-Ler-F	CAGGCTGGAGAGATGACAAAA
GT-FLC-Ler-R	AAACAATCTGGACAGTAGAGGCTTAT
GT-FLC-Rep-F	ATTAAATCATAATTAAGACCAGGAG
GT-FLC-Rep-R	AAATGTAAGCCACATTAATTGGGAAA
ChIP-ACT-F	ACTCGTTTCGCTTTCCTTAGTGTTAGCTG
ChIP-ACT-R	AGCGAACGGATCTAGAGACTCACCTTG
ChIP-FLC-a-F	GCGGACTCACGTTAGTCATGGGTAGGG
ChIP-FLC-a-R	GAACTTGGATTGATGTGGGGCACTATTAAG
ChIP-FLC-b-F	AGGTTTGGGTTCAAGTCGCCGGAGATACTA
ChIP-FLC-b-R	CTGGCCCGACGAAGAAAAAGTAGATAGGCA
ChIP-FLC-c-F	GAGAAACAACAAGAGATCCGCCGGAAAA
ChIP-FLC-c-R	AACCAAATTTAAGGAAGAACAATGTCGTGA

ChIP-FLC-d-F	CGGTAAGTACTAATTGTGAGGCTGAGTTT
ChIP-FLC-d-R	CTATGAATTCCTATCTTTGCTGTGGACCTA
ChIP-FLC-e-F	GGCCACTGGAAACTATGAAACATTGAG
ChIP-FLC-e-R	TGTTTTTCTGAAATGTTACGAATACTAGCG
ChIP-FWA- a-F	AGAGCGCCACAGCTTCAG
ChIP-FWA- a-R region	ATGCAGCTGATGTGCCTT
ChIP-FWA- a-Probe	FAM-ATGCAGCTGATGTGCCTT
ChIP-FWA-b-F	CTCATATATTCTTTATCGAAGCCCATACATCTT
ChIP-FWA-b-R	GCGCTCGTATGAATGTTGAATGG
ChIP-FWA-b-Probe	CCGTCGAGAATCTCA
In situ-TEK-F	GCCGTTGAGATCAGCTCAGGTTG
In situ-TEK-R	CGACATGACACGCTGCGCAGG
order# 185478162	At02329915_s1. Control for Taqman RT-PCR
Bs-AtMu1-F	CTCTTTCATTCAAATTTTAATTTTTTCCATAACAAAART
Bs-AtMu1-R	AATATATATAATTTTACGTAATTAATTAATATTAATYAAG
RT-AGL24-F	GAGGCTTTGGAGACAGAGTCGGTGA
RT-AGL24-R	AGATGGAAGCCCAAGCTTCAGGGAA
RT-FVE-F	AGTGGTCTCCTGATAAGTCATCCGTCTTTG
RT-FVE-R	CAGACTTCTTACTGACCCTGTCATAATCCC
RT-FLD-F	GGTCTTGGTGTTGGAGCTGATTCAGTCATT
RT-FLD-R	TTTTGTGCCTGAGGTAGATGATGATGGTAG
RT-FRL1-F	AAGGCATTGAGGAAACGCAACACGACTAAT
RT-FRL1-R	TCTAGAAAGTAGCTGCTGACTCGGAACTGG
RT-FRL2-F	GCCCACCGTACTATCCTCAGTAGCATCT
RT-FRL2-R	GCAGAAATCTTCTCAATATCGCTTGCATTC
RT-AHL15-F	GCAGCCGCCGATGTATAATATGCC
RT-AHL15-R	CAATACGAAGGAGGAGCACGAGG
RT-AHL17-F	GGAAGTGGAGGAGAGTCGTGTG
RT-AHL17-R	GTATGGCGGTGGAGCTCTGGC
RT-AHL18-F	GCGACATCGTTTATTGGGTCGCC
RT-AHL18-R	CGGTCGTTGCGTTCCCCAATAAG
RT-AHL19-F	GGCGGAGGTTCGCCACTAAGC
RT-AHL19-R	GCCGCTCATCTGTCCTCCTCC
RT-AHL20-F	GTGACTCACCGCCCAGAATCGG
RT-AHL20-R	GGTTCGTGCCCTAGCTGACCAG
RT-AHL24-F	CATTGGAGTCGCCGCCAATGATG
RT-AHL24-R	ACGGTGGTCGTCCCGTTGACC
RT-AHL25-F	GCCCAGGCGTGTGAGTCAAACC
RT-AHL25-R	GTCTAGTCGCACCGCCACCAC
RT-AHL27-F	CAGGGACAGTTAGGAGGTAATGTGG
RT-AHL27-R	GGTGGTCTTGAAGGTGTTCCAGC
RT-AHL28-F	GGACAATCGCCGCCGGTCTC
RT-AHL28-R	CAGTACGGCGATGGAGCTTTGG

RT-AHL29-F	CCACCATCTGGAGCCGGTCAAG
RT-AHL29-R	GGTCTTGGTGGTGCGGCTGC
RT-GIK1-F	GTATCTCCACTTACGCTCGTCGG
RT-GIK1-R	GTACCCCGCAGAGTCACAACAG
RT-AT1G31580-F	ATTGTCCCCATTCATGTTCC
RT-AT1G31580-R	TCAGTGACTTGGTGAGTTTTTTG
RT-AT1G33370-F	GCACCAATGGTTCAGTGGTAG
RT-AT1G33370-R	TACACCGTCTGGGATCGAA
RT-AT2G01422-F	ATCCATCCAAGGCAGAAGC
RT-AT2G01422-R	GAGTGAGAGCCTCATGAAGGA
RT-AT2G13431-F	CTTTTACCCAGGTGAGCAAAC
RT-AT2G13431-R	CAAGCTCTTAACGCAAATTCAAG
RT-AT2G17690-F	TCTCTGGGAAGATGGTAATGGCA
RT-AT2G17690-R	AACCTATCGTTTTGGGAGGGTCA
RT-AT3G29639-F	TGGAAACCAGAAAGCAAAGAG
RT-AT3G29639-R	CCACAGACACAGAAACTCATATACAG

RT	Real-time PCR primers for cDNA expression analysis
GT	Genotyping PCR primers
ChIP	Real-time PCR primers for ChIP analysis
Probe	Primers for TE fragment for Southern Blots probe
In situ	Primers for cDNA fragment for in situ probe
Bs	Primers for Bisulfite sequencing

Table S4

Oligonucleotide sequences used in this study

Supplemental Experimental Procedures

Plant materials, DNA constructs and growth conditions

The plants used for expression analysis in this study were grown at 22°C under 16-h light/8 h dark cycle. For the flowering phenotype shown in Figure 1, the plants were grown at 22°C under continuous light growth condition. Transgenic plants were generated by *Agrobacterium*-mediated infiltration [4]. The amiRNA constructs were designed based on the Web MicroRNA Design platform [5] and engineered into pGreen Vector [6] with tandem 35S enhancers. The cassettes containing *35S-amiTEK*-Nos terminator was recloned into *pBGW* binary vector using gateway cloning [7]. For *pTEK::TEK-GUS* construction, *TEK* genomic fragment (from –2385 to +1882; A of the start codon ATG was set as +1), which included a 2.4 kb promoter, 1.1 kb downstream plus a 774 bp genomic coding region, was used for gateway cloning. The inflorescence was stained in a staining solution with 2.0 mM 5-bromo-4-chloro-3-indolyl-β-d-glucuronic acid (X-Gluc) at 37ºC for 8 h. Oligonucleotide sequences are listed in Table S4.

Vernalization treatments were performed as described [8] with modification. Seeds were germinated on Murashige and Skoog (MS, Sigma) plates and the seedlings were kept at room temperature one day to allow plants to become metabolically active. Then, the plants were transferred to 4°C for 42 days, and thereafter were transferred back to 22°C for 4 days, and then the whole plants including the roots were harvested for RNA extraction.

RNA extraction and expression analysis

For the expression analysis of *TEK*, total RNA was isolated from roots, rosette leaves, stems, vegetative shoot apical meristems, inflorescence meristems, young flower buds, siliques and open flowers. T3 plants of two independent *amiTEK* lines with strong late flowering phenotypes, namely line 2 and line 21, were used for the expression analysis in the wild-type L*er* and the *amiTEK* plants. The aerial part of the plants without roots were harvested just before the lights were off at DAG 5, 7, 9, 11, 13, and 15. The RNeasy plant mini kit (Qiagen) was used for RNA extraction and the Superscript III RT-PCR system (Invitrogen) was used for reverse-transcription. Three biological replicates were taken for the calculation of standard deviation. Quantitative real-time PCR assays were performed in triplicate with the 7900HT fast real-time PCR system (Applied Biosystems) using the SYBR Green PCR master mix (Applied Biosystems). Statistical analysis was done using paired Student's *t*-test based on all the data. *Tubulin 2 (TUB2)* was used as a control. Primer sequences are shown in Table S4.

In situ hybridization

Nonradioactive in situ hybridization was performed as described [9]. A 3′- specific region of *TEK* cDNA were amplified by PCR and cloned into *pCRII-TOPO* vector *(Invitrogen)*, and used as templates for sense and anti-sense probe synthesis by in vitro transcription (Roche). Primer sequences are shown in Table S4.

ChIP assays

The ChIP assay was performed as described [10, 11] with some modifications. For histone modifications, the aerial tissues of plants at DAG 5 and 15 were used. For the TEK binding assay, inflorescences and leaves of *35S::TEK-HA* in L*er* and *pTEK::TEK-YFP* in Col which can rescue were used. *35S::TEK-HA* is functional and can prevent the effect of *35S::amiTEKb* as *35S::TEK*-HA does not contain the target site of *amiTEKb*. *pTEK::TEK-YFP* can rescue the sterile phenotype of *tek-1*. Chromatin was solubilized by sonication to an average DNA length of 300 bp, and incubated overnight with anti-modified histone (Upstate) for H3K9me2, acetylated histone H3, H3K27me3 and H3 as a control. The relative enrichment for the histone modification experiments was the ratio obtained from $(B_{Sp}/C_{Sp})/(B_{Ctrl}/C_{Ctrl})$, where B and C are amount of bound DNA with a specific antibody and with control H3 antibody, respectively. Sp, measured by a specific primer pair. Ctrl, measured by a control primer pair (*ACT*). The relative enrichment for HA- or YFP-tagged TEK ChIP experiments was the ratio obtained from$[(B_{Sp}/I_{Sp})/(B_{Ctrl}/I_{Ctrl})$ using the HA or YFP antibody (Upstate)]/ $[(B_{Sp}/I_{Sp})/(B_{Ctrl}/I_{Ctrl})$ using the control myc antibody], where B and I are amount of bound DNA and input DNA, respectively, measured by specific or control (ACT) primer pairs. The control value was normalized to 1.0. At least three independent biological replicates of ChIP assay were performed. SYBR Green and TaqMan Real-time PCR assays were done in triplicate for *FLC* and *FWA* loci, respectively. Primer sequences are shown in Table S4.

Matrix association assay

Nuclear matrix associated DNA and free DNA were isolated as described previously [9]. The purified DNA was quantified by real-time PCR and the ratio of free DNA to matrix DNA was calculated as $(F_{Sp}/M_{Sp})/(F_{Ctrl}/M_{Ctrl})$, where F and M are amount of Free and Matrix DNA, respectively, measured by specific or control (*ACT*) primer pairs. Primer sequences are shown in Table S4.

Microarray analysis & RNA sequencing

The NimbleGen 4x72K arrays were used for global expression analysis. The wild-type L*er* and T3 plants of the *amiTEK* were grown at MS medium plates and harvested at DAG 5. Total RNA was extracted from whole seedlings including the roots with the RNeasy plant mini kit (Qiagen) and the double-stranded cDNAs were synthesized with the Invitrogen Superscript Double-Stranded cDNA synthesis Kit, and then were hybridized to the array following NimbleGen's protocols. Two biological replicates were used, giving two WT samples and two *amiTEK* samples, which are compared with each other individually; thus there are a total of 4 comparisons in total. The software ArrayStar (DNAStar Inc.) was used for the data analysis and $p<0.05$. TAIR7 release of Arabidopsis genome was used for annotations of genes and transposon/pseudo genes. The raw data are deposited in NCBI's Gene Expression Omnibus and are accessible through the GEO Super Series accession number GSE39158.

RNA sequencing libraries were constructed per manufacturer instructions (Illumina) and sequenced with an Illumina HiSeq 2000. Sequencing reads were mapped with Bowtie [12]. Gene and transposon expression in the RNA-seq data was measured by calculating reads per kilobase

per million mapped reads (RPKM). P-values to detect differential expression were calculated by Fisher's exact test and Benjamini-Hochberg corrected for multiple testing. Genes and TEs differentially expressed were defined as those with *tek-1*/wild type>4 and P<0.05.

Southern blot analysis and Genotyping PCR analysis

Genomic DNA was extracted from DAG 10 wild-type L*er* seedlings or vegetative tissues of individual DAG 30 *amiTEK* plants with DNeasy plant mini kit (QIAGEN). For the Southern blot analysis, about 1 μg of genomic DNA digested with *EcoRV* (for *Mutator*-like TE) or *EcoRI* (for *CACTA*-like and *hAT*-like TE) was separated on 0.8% agarose gels, blotted onto Nylon membranes (Roche) and hybridized with the DIG-labeled (Roche) probes, which correspond to the specific region of the *Mutator*-like insertion in L*er FLC* intron 1 (around 500 bp), *CACTA*-like and *hAT*-like fragments (around 150 bp). The filter was washed with 0.1 x SSC and 0.1% (w/v) SDS at 68 ºC. The signal was made visible with chemi-luminescent detection kit using anti-DIG antibodies (Roche).

To distinguish L*er FLC* and Col *FLC*, PCR of genomic DNA was amplified with primers α and β, followed by *Taq*1 restriction digestion, as L*er FLC* showed a band of 342 bp and 287 bp, while Col *FLC* showed 372 bp and 287 bp. The primers γ and δ amplified a 1,741-bp fragment with the TE insertion from the control L*er* plants, and a 527-bp fragment from the control Col plants.

Bisulfite genomic sequencing

DNA was extracted from DAG 10 seedlings of wild type and of *amiTEK*, and subsequently, about 0.2-µg genomic DNA was treated with bisulfite using the EpiTect Bisulfite kit (Qiagen) according to the manufacturer's instructions. Following the bisulfite conversion, the bottom strands of *FWA* (tandem-repeat region) and *AtMu1* (the 3' terminal-inverted-repeat region) were amplified by PCR, and cloned into the *T-Easy* vector (Promega). For each genotype, at least 15 individual clones were sequenced and examined. Primer sequences are shown in Table S4.

Yeast two-hybrid and bimolecular fluorescence complementation assay

For the yeast two-hybrid assay, the full-length coding sequences for TEK, CURLY LEAF (CLF), VERNALIZATION2 (VIN2), EMBRYONIC FLOWER2 (EMF2), FERTILIZATION-INDEPENDENT ENDOSPERM (FIE), LIKE HETEROCHROMATIN 1 (LHP1), EMBRYONIC FLOWER 1 (EMF1), HISTONE DEACETYLASE 19 (HDA19), FVE and MSI5 were cloned in the Matchmaker GAL4 Two-Hybrid System 3 (BD Clontech) according to the manufacturer's instructions. For the fluorescence assay, the same full-length TEK, FVE and MSI5 were translationally fused with either an N-terminal or a C-terminal EYFP fragment-containing vectors (www.bio.purdue.edu/people/faculty/gelvin/nsf/index.htm). Using the Helium biolistic gene transformation system (Bio-Rad), onion epidermal cells were transiently co-transformed with plasmids. Within 24-48 hours after bombardment, EYFP fluorescence in the onion cells was observed and imaged using a Zeiss LSM 5 EXCITER upright laser scanning confocal microscopy.

Co-immunoprecipitation assay

Co-immunoprecipitation was carried out as described previously [13]. Briefly, total proteins were extracted from about 10 day-old F1 seedlings; subsequently, the protein extracts were incubated and precipitated with anti-FLAG M2 affinity gel (Sigma). The precipitates were washed for three times and boiled with an SDS-PAGE loading buffer. Immunoprecipitated proteins were detected via western blotting with anti-FLAG and anti-YFP (Upstate).

Supplemental References

1. **To, T.K., Kim, J.M., Matsui, A., Kurihara, Y., Morosawa, T., Ishida, J., Tanaka, M., Endo, T., Kakutani, T., Toyoda, T., et al. (2011). Arabidopsis HDA6 regulates locus-directed heterochromatin silencing in cooperation with MET1. PLoS Genet *7*, e1002055.**
2. **Zhang, X., Yazaki, J., Sundaresan, A., Cokus, S., Chan, S.W., Chen, H., Henderson, I.R., Shinn, P., Pellegrini, M., Jacobsen, S.E., et al. (2006). Genome-wide high-resolution mapping and functional analysis of DNA methylation in arabidopsis. Cell *126*, 1189-1201.**
3. **Zilberman, D., Gehring, M., Tran, R.K., Ballinger, T., and Henikoff, S. (2007). Genome-wide analysis of Arabidopsis thaliana DNA methylation uncovers an interdependence between methylation and transcription. Nat Genet *39*, 61-69.**
4. **Clough, S.J., and Bent, A.F. (1998). Floral dip: a simplified method for Agrobacterium-mediated transformation of Arabidopsis thaliana. Plant Journal *16*, 735-743.**
5. **Schwab, R., Ossowski, S., Riester, M., Warthmann, N., and Weigel, D. (2006). Highly specific gene silencing by artificial microRNAs in Arabidopsis. Plant Cell *18*, 1121-1133.**
6. **Hellens, R.P., Edwards, E.A., Leyland, N.R., Bean, S., and Mullineaux, P.M. (2000). pGreen: a versatile and flexible binary Ti vector for Agrobacterium-mediated plant transformation. Plant Mol Biol *42*, 819-832.**
7. **Karimi, M., Inze, D., and Depicker, A. (2002). GATEWAY((TM)) vectors for Agrobacterium-mediated plant transformation. Trends Plant Sci *7*, 193-195.**

8. Michaels, S.D., and Amasino, R.M. (2001). Loss of FLOWERING LOCUS C activity eliminates the late-flowering phenotype of FRIGIDA and autonomous pathway mutations but not responsiveness to vernalization. Plant Cell *13*, 935-941.

9. Ng, K.H., Yu, H., and Ito, T. (2009). AGAMOUS controls GIANT KILLER, a multifunctional chromatin modifier in reproductive organ patterning and differentiation. PLoS biology *7*, e1000251.

10. Ito, T., Takahashi, N., Shimura, Y., and Okada, K. (1997). A serine/threonine protein kinase gene isolated by an in vivo binding procedure using the Arabidopsis floral homeotic gene product, AGAMOUS. Plant & cell physiology *38*, 248-258.

11. Sun, B., Xu, Y., Ng, K.H., and Ito, T. (2009). A timing mechanism for stem cell maintenance and differentiation in the Arabidopsis floral meristem. Genes Dev *23*, 1791-1804.

12. Langmead, B., Trapnell, C., Pop, M., and Salzberg, S.L. (2009). Ultrafast and memory-efficient alignment of short DNA sequences to the human genome. Genome biology *10*, R25.

13. Gu, X., Jiang, D., Yang, W., Jacob, Y., Michaels, S.D., and He, Y. (2011). Arabidopsis homologs of retinoblastoma-associated protein 46/48 associate with a histone deacetylase to act redundantly in chromatin silencing. PLoS Genet *7*, e1002366.